



## ICTM: an interval tessellation-based model for reliable topographic segmentation

Marilton Sanhotene de Aguiar \*, Graçaliz Pereira Dimuro and  
Antônio Carlos da Rocha Costa \*

*Escola de Informática, Universidade Católica de Pelotas, 96010-000, Pelotas, Brazil*  
E-mail: {marilton;liz;rocha}@ucpel.tche.br

This work introduces a tessellation-based model for the declivity analysis of geographic regions. The analysis of the relief declivity, which is embedded in the rules of the model, categorizes each tessellation cell, with respect to the whole considered region, according to the (positive, negative, null) sign of the declivity of the cell. Such information is represented in the states assumed by the cells of the model. The overall configuration of such cells allows the division of the region into subregions of cells belonging to a same category, that is, presenting the same declivity sign. In order to control the errors coming from the discretization of the region into tessellation cells, or resulting from numerical computations, interval techniques are used. The implementation of the model is naturally parallel since the analysis is performed on the basis of local rules. An immediate application is in geophysics, where an adequate subdivision of geographic areas into segments presenting similar topographic characteristics is often convenient.

**Keywords:** tessellation-based model, topographic categorization, interval mathematics, geophysics

**AMS subject classification:** 68U99, 65G40, 86A04, 65G20

### 1. Introduction

In [1], it is proposed a general tessellation-based model for categorizer tools that are able to subdivide a certain geographic region into subregions presenting similar characteristics, that is, belonging to the same range concerning a set of given observable properties. The number of the characteristics that should be studied determines the number of layers of the model. In each layer, a probably different analysis of the region is obtained. An appropriate projection of all layers into the base layer of the model leads to a meaningful subdivision of the region and a categorization of the subregions that consider the simultaneous occurrence of all characteristics, according to some priorities. To control the errors coming from discretization and resulting from the numerical computations, interval techniques [7] are used to obtain a reliable categorization. This model is called an *Interval Categorizer Tessellation-Based Model (ICTM)*.

---

\* M.S. de Aguiar and A.C.R. Costa are also at Programa de Pós-Graduação em Computação, Universidade Federal do Rio Grande do Sul, 91.501-970, Porto Alegre, Brazil.

In this paper, we present the so-called Topo-ICTM, which is a bi-dimensional 1-layer ICTM to analyze the variation of declivity signal of the function that maps the topography of a given region, subdividing this region into subregions presenting the same behavior with respect to declivity of the relief. Each such subregion is said to belong to a given declivity category according to the (positive, negative, null) sign of the declivity of the relief function.<sup>1</sup> An immediate application is in Geophysics, where an adequate subdivision of geographic areas into segments presenting similar characteristics is often convenient [2].

To automate this kind of topological analysis based on the proposed model, we have developed the system Topo-ICTM, implemented in C/C++ (Linux). An envisaged application is to help in survey activities concerning oil exploitation in the basin of Pelotas, which is classified as of high risk due to the nature of its geological data.

There are many methods for image segmentation [3,4,6,8] and the most commonly used techniques can be classified into two categories: (i) *region extraction techniques*, which look for maximal regions satisfying some homogeneity criterion, and (ii) *edge extraction techniques*, which look for edges occurring between regions with different characteristics. The main problem with most of these methods is that they are heuristic and frequently different methods give different results, and, therefore, it is desirable to produce reliable methods (see, e.g, [2,9]).

The model presented in this paper evolved directly from the analysis of [2], which has presented a method that is based in a one-dimensional analysis to subdivide geophysical areas into monotonicity subregions, considering just one direction. The tessellation-based model presented here performs a bi-dimensional analysis of the declivity, using local rules for the creation and categorization of subregions, giving the relative situation of each subregion with respect the whole area, according to the states assumed by the tessellation cells. The analysis can be easily refined either to focus a subregion of a certain declivity category, or to change the input parameters (number of tessellation cells, etc.), or to consider a cell neighborhood of larger radium, for instance.

The paper is organized as follows. Section 2 introduces the matrix operations that define the behavior of Topo-ICTM. It is subdivided into subsections describing the steps of the categorization process. Section 3 presents the conclusion and further work.

## 2. The formalization of the Topo-ICTM model

This section introduces the interval categorizer tessellation-based model for the declivity-based categorization of a topographic region, called Topo-ICTM, formalized in terms of matrix operations. The data input for the model are extracted from satellite photos of the geographic region being analyzed, where the heights are given in certain points referenced by their latitude and longitude coordinates. This geographic region is represented by a regular tessellation that is determined by subdividing the total area into

---

<sup>1</sup> In this paper, whenever it can be understood from the context, we may use the term “declivity” to mean “signal of the declivity function”.

sufficiently small rectangular subareas, each one represented by one cell of the tessellation. This subdivision is done according to a cell size established by the geophysics analyst and it is directly associated to the refinement degree of the tessellation.

**Definition 1.** A *tessellation* is a matrix  $M$  with  $n_r$  rows and  $n_c$  columns. The entry at the  $x$ th row and the  $y$ th column is called the  $xy$ -cell of  $M$ .

### 2.1. The interval spectrum matrices

In topographic analysis, usually there are too much data, most of which is geophysically irrelevant. We then take, for each subdivision, the average value of the heights at the points supplied by the satellite photos, which are the entries of the spectrum matrix of the tessellation  $M$ .

**Definition 2.** The *spectrum matrix* of a tessellation  $M$  is the  $n_r \times n_c$  matrix  $M^{\text{abs}} = [m_{xy}^{\text{abs}}]$ , where the entry  $m_{xy}^{\text{abs}}$  is the absolute value of the average height of the points represented by the  $xy$ -cell of  $M$ .

We are interested in comparing the spectral values corresponding to different cells, so we are not interested in absolute values, only in relative ones. To simplify the data of the spectrum matrix, we normalize them by dividing each  $m_{xy}^{\text{abs}}$  by the largest  $m_{\text{max}}$  of these values.

**Definition 3.** The *relative spectrum matrix*  $M^{\text{rel}}$  is defined as the  $n_r \times n_c$  matrix given by  $M^{\text{rel}} = M^{\text{abs}}/m_{\text{max}}$ .

The heights are measured pretty accurately, so the only errors in the values  $m_{xy}$  come from the discretization of the area in terms of the discrete set of tessellation cells. In other words, it is desirable to know the values of the relief function  $h_{\xi\nu}$  for all  $\xi$  and  $\nu$ , but only the values  $h_{xy} \equiv m_{xy}^{\text{rel}} = m_{xy}^{\text{abs}}/m_{\text{max}}$  for  $11, \dots, 1n_r, \dots, n_c1, \dots, n_cn_r$ , determined by division of the region in  $n_r n_c$  cells, are used in the effective calculations.

In the following, we apply interval mathematics techniques to control the errors associated to the cell values.<sup>2</sup> For each  $\xi\nu$ , which is different from  $xy$ , it is reasonable to estimate  $h_{\xi\nu}$  as the value  $m_{xy}^{\text{rel}}$  at the point  $xy$  which is closest to  $\xi\nu$ , meaning that  $\xi\nu$  belongs to the same segment of area as  $xy$ . For each cell  $xy$ , let  $\Delta_x$  and  $\Delta_y$  be the largest possible errors of the corresponding approximations considering the west–east direction and the north–south direction, respectively.

For fixed  $y$ , when  $\xi > x$ , the point  $xy$  is still the closest until we reach the midpoint  $x_{\text{mid}}y = ((x + (x + 1))/2)y$  between  $xy$  and  $(x + 1)y$ . It is reasonable to assume that the largest possible approximation error  $|m_{xy}^{\text{rel}} - h_{\xi y}|$  for such points is attained when the distance between  $xy$  and  $\xi y$  is the largest, i.e., when  $\xi y = x_{\text{mid}}y$ . In this case, the approximation error is equal to  $|h_{x_{\text{mid}}y} - m_{xy}^{\text{rel}}|$ .

<sup>2</sup> To see examples of the advantages of using intervals in solving similar problems see, e.g., [2,5].

**Lemma 1.** For fixed  $y$ , if  $\xi > x$ , then the approximation error  $\epsilon$  is bounded by  $0.50 \times |m_{(x+1)y}^{\text{rel}} - m_{xy}^{\text{rel}}|$ .

*Proof.* If the points  $xy$  and  $(x+1)y$  belong to the same segment of area, then the dependence of  $n_{\xi y}$  on  $\xi y$  should be reasonably smooth for  $\xi \in [x, (x+1)]$ . On a narrow interval  $[x, (x+1)]$ , we can, with reasonable accuracy, ignore the quadratic and higher terms in the expansion of  $h_{(\xi+\Delta\xi)y}$  and approximate  $h_{\xi y}$  by a linear function. For a linear function  $\xi \mapsto h_{\xi y}$ , the difference  $h_{x_{\text{mid}}y} - m_{xy}^{\text{rel}}$  is equal to the half of the difference  $m_{(x+1)y}^{\text{rel}} - m_{xy}^{\text{rel}}$ . On the other hand, if the points  $xy$  and  $(x+1)y$  belong to different segments, then the dependence  $h_{\xi y}$  should exhibit some non-smoothness, and it is reasonable to expect that the difference  $m_{(x+1)y}^{\text{rel}} - m_{xy}^{\text{rel}}$  is much higher than the approximation error. In both cases, the approximation error  $\epsilon$  is bounded by  $0.50 \times |m_{(x+1)y}^{\text{rel}} - m_{xy}^{\text{rel}}|$ .  $\square$

**Lemma 2.** For fixed  $y$ , if  $\xi < x$ , then the approximation error  $\epsilon$  is bounded by  $0.50 \times |m_{xy}^{\text{rel}} - m_{(x-1)y}^{\text{rel}}|$ .

**Proposition 1.** For the approximation error  $\epsilon_x$ ,

$$\epsilon_x \leq \Delta_x = 0.5 \cdot \min(|m_{xy}^{\text{rel}} - m_{(x-1)y}^{\text{rel}}|, |m_{(x+1)y}^{\text{rel}} - m_{xy}^{\text{rel}}|).$$

*Proof.* It follows from lemmas 1 and 2.  $\square$

As a result, considering a given  $y$ , besides of the central values  $m_{xy}^{\text{rel}}$ , for each  $x$ , we get intervals  $m_{xy}^{x[1]}$  containing all the possible values of  $h_{\xi y}$ , for  $x - \frac{1}{2} \leq \xi \leq x + \frac{1}{2}$ .

**Corollary 1.** Considering a fixed  $y$ , for each  $x$ , if  $x - \frac{1}{2} \leq \xi \leq x + \frac{1}{2}$ , then  $h_{\xi y} \in m_{xy}^{x[1]} = [m_{xy}^{x-}, m_{xy}^{x+}]$ , where  $m_{xy}^{x-} = m_{xy}^{\text{rel}} - \Delta_x$  and  $m_{xy}^{x+} = m_{xy}^{\text{rel}} + \Delta_x$ .

Using an analogous argumentation, for a fixed  $x$ , it follows that:

**Proposition 2.** For the approximation error  $\epsilon_y$ ,

$$\epsilon_y \leq \Delta_y = 0.5 \cdot \min(|m_{xy}^{\text{rel}} - m_{x(y-1)}^{\text{rel}}|, |m_{x(y+1)}^{\text{rel}} - m_{xy}^{\text{rel}}|).$$

**Corollary 2.** Considering a fixed  $x$ , for each  $y$ , if  $y - \frac{1}{2} \leq v \leq y + \frac{1}{2}$ ,  $h_{xv} \in m_{xy}^{y[1]} = [m_{xy}^{y-}, m_{xy}^{y+}]$ , where  $m_{xy}^{y-} = m_{xy}^{\text{rel}} - \Delta_y$  and  $m_{xy}^{y+} = m_{xy}^{\text{rel}} + \Delta_y$ .

**Definition 4.** If  $m_{xy}^{x\pm} = m_{xy}^{\text{rel}} \pm \Delta_x$  and  $m_{xy}^{y\pm} = m_{xy}^{\text{rel}} \pm \Delta_y$ , the *interval spectrum matrices*  $M^{x[1]}$  and  $M^{y[1]}$ , associated with the relative spectrum matrix  $M^{\text{rel}}$ , are defined, respectively, by the  $n_r \times n_c$  interval matrices

$$M^{x[1]} = [m_{xy}^{x[1]}] = [[m_{xy}^{x-}, m_{xy}^{x+}]] \quad \text{and} \quad M^{y[1]} = [m_{xy}^{y[1]}] = [[m_{xy}^{y-}, m_{xy}^{y+}]].$$

## 2.2. The declivity registers and the state matrix

We proceed to a declivity categorization inspired by [2]. We assume from the start that the relief approximation functions introduced by the tessellation-based model are piecewise linear functions. We cast the whole process as a kind of constraint satisfaction problem, where the tessellation-based model is in charge of finding a piecewise linear relief approximation function (and corresponding set of limit points between the resulting subregions) that fits the constraints imposed by the interval spectrum matrix. To narrow the solution space to a minimum, we take a qualitative approach to the relief approximation functions, clustering them in equivalence classes according to the sign of their declivity (positive, negative, null), thus making the tessellation-based model build a single qualitative solution to that constraint satisfaction problem, namely, the class of approximation functions compatible with the constraints of the interval spectrum matrix. We proceed as follows:

**Proposition 3.** Let  $M^{x^{[1]}}$  and  $M^{y^{[1]}}$  be interval spectrum matrices. For a given  $xy$ , if:

- (i)  $m_{xy}^{x^+} \geq m_{(x+1)y}^{x^-}$ , then there exists a non-increasing relief approximation function between  $xy$  and  $(x+1)y$  (direction west–east).
- (ii)  $m_{(x-1)y}^{x^-} \leq m_{xy}^{x^+}$ , then there exist a nondecreasing relief approximation function between  $(x-1)y$  and  $xy$  (direction west–east).
- (iii)  $m_{xy}^{y^+} \geq m_{x(y+1)}^{y^-}$ , then there exists a non-increasing relief approximation function between  $xy$  and  $x(y+1)$  (direction north–south).
- (iv)  $m_{x(y-1)}^{y^-} \leq m_{xy}^{y^+}$ , then there exists a nondecreasing relief approximation function between  $x(y-1)$  and  $xy$  (direction north–south).

*Proof.* A sketch of the proof is given. In (i), take, for example,  $\mu_{xy} = m_{xy}^{x^+}$ ,  $\mu_{(x+1)y} = m_{(x+1)y}^{x^-}$  and use a linear interpolation to define the values  $\mu_{ky}$  for  $x < k < x+1$ . The proofs of (ii)–(iv) are similar.  $\square$

For each cell, four directed declivity registers<sup>3</sup> – *reg.e* (east), *reg.w* (west), *reg.s* (south) and *reg.n* (north) – are defined, indicating the admissible sign declivity of the function that approximates the relief function in any of these directions, taking into account the values of the neighbor cells. The analysis of declivity is done according to proposition 3.

**Definition 5.** A *declivity register* of an  $xy$ -cell is a tuple  $reg = (reg.e, reg.w, reg.s, reg.n)$ , where the values of the directed declivity registers are given by:

<sup>3</sup> This paper uses the dot notation of the object-oriented programming languages to represent the components of a data structure (e.g., *reg.e* denotes the component *e* of the data structure *reg*).

- (a) For non border cells, considering the conditions given by proposition 3:  $reg.e = 0$ , if 3(i) holds;  $reg.w = 0$ , if 3(ii) holds;  $reg.s = 0$ , if 3(iii) holds;  $reg.n = 0$ , if 3(iv) holds;  $reg.e, reg.w, reg.s, reg.n = 1$ , otherwise.
- (b) For east, west, south and north border cells:  $reg.e = 0, reg.w = 0, reg.s = 0$  and  $reg.n = 0$ , respectively.<sup>4</sup> The other directed declivity registers of border cells are also determined according to item (a).

**Definition 6.** The *declivity register matrix* is defined as an  $n_r \times n_c$  matrix  $M^{reg} = [m_{xy}^{reg}]$ , where the entry at the  $x$ th row and the  $y$ th column is the value of the declivity register of the corresponding cell.

**Corollary 3.** Considering the west–east direction, any relief approximation function  $m_{xy}$  is either (i) strictly increasing between  $xy$  and  $(x + 1)y$  if  $m_{xy}^{reg.e} = 1$  (in this case,  $m_{(x+1)y}^{reg.w} = 0$ ); or (ii) strictly decreasing between  $xy$  and  $(x + 1)y$  if  $m_{(x+1)y}^{reg.w} = 1$  (in this case,  $m_{xy}^{reg.e} = 0$ ); or (iii) constant between  $xy$  and  $(x + 1)y$  if  $m_{xy}^{reg.e} = 0$  and  $m_{(x+1)y}^{reg.w} = 0$ . Similar results hold for the north–south direction.

**Definition 7.** Let  $w_{reg.e} = 1, w_{reg.s} = 2, w_{reg.w} = 4$  and  $w_{reg.n} = 8$  be weights to be associated to the directed declivity registers. The *state matrix* is defined as an  $n_r \times n_c$  matrix given by  $M^{state} = [m_{xy}^{state}]$ , where the entry at the  $x$ th row and the  $y$ th column is the value of the corresponding cell state, calculated as the value of the binary encoding of the corresponding directed declivity registers, given as

$$m_{xy}^{state} = w_{reg.e} \times m_{xy}^{reg.e} + w_{reg.s} \times m_{xy}^{reg.s} + w_{reg.w} \times m_{xy}^{reg.w} + w_{reg.n} \times m_{xy}^{reg.n}.$$

Thus, for given  $xy$ , the correspondent cell can assume one and only one state presented in figure 1, represented by the value  $m_{xy}^{state} = 0, \dots, 15$ .

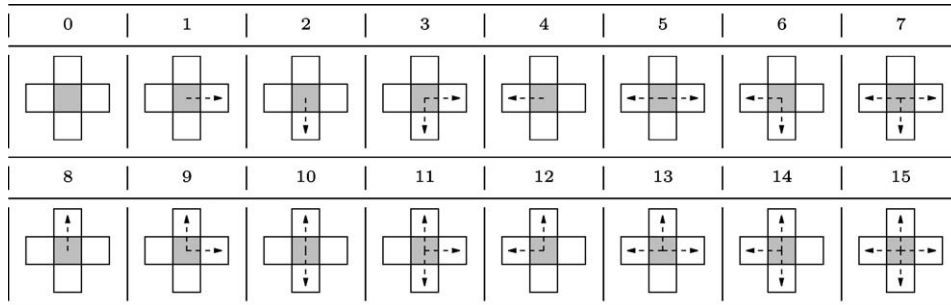


Figure 1. The schema of the all possible cell state values.

<sup>4</sup> This is consistent with the relief function being a constant in the border cells.

Table 1  
Conditions of non limiting cells  $xy$ .

Id	Conditions
1	$m_{(x-1)y}^{reg.e} = m_{xy}^{reg.e} = 1$
2	$m_{xy}^{reg.w} = m_{(x+1)y}^{reg.w} = 1$
3	$m_{(x-1)y}^{reg.e} = m_{xy}^{reg.e} = m_{xy}^{reg.w} = m_{(x+1)y}^{reg.w} = 0$
4	$m_{x(y-1)}^{reg.s} = m_{xy}^{reg.s} = 1$
5	$m_{xy}^{reg.n} = m_{x(y+1)}^{reg.n} = 1$
6	$m_{x(y-1)}^{reg.s} = m_{xy}^{reg.s} = m_{xy}^{reg.n} = m_{x(y+1)}^{reg.n} = 0$

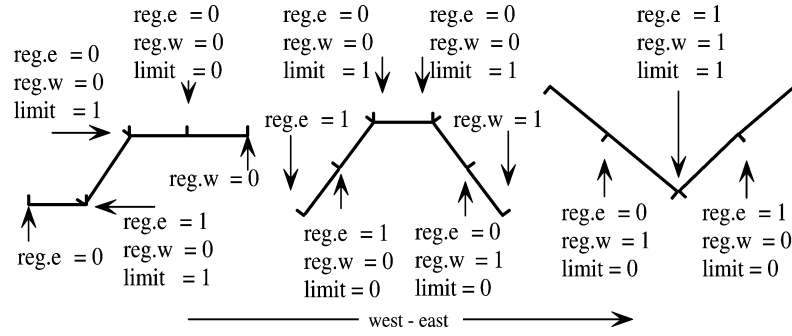


Figure 2. Schemas of limiting cells.

### 2.3. The limiting matrix and the constant-declivity subregions

A *limiting cell* is defined as the one where the relief function changes its declivity, presenting critical points (maximum, minimum or inflection points). To identify such limiting cells, we use a limiting register associated to each cell. The border cells are assumed to be limiting.

**Definition 8.** The *limiting matrix* is defined as the  $n_r \times n_c$  matrix given by  $M^{\text{limit}} = [m_{xy}^{\text{limit}}]$ , where the entry at the  $x$ th row and the  $y$ th column is determined as  $m_{xy}^{\text{limit}} = 0$ , if one of the conditions listed in table 1 holds, and  $m_{xy}^{\text{limit}} = 1$ , otherwise.

Analyzing the limiting matrix it is easy to detect the existence of known relief configurations (see, e.g., figure 2). The presence of limiting cells allows the subdivision of the whole area into declivity categories.

**Definition 9.** The *constant declivity subregion* associated to the non limiting cell  $xy$ , denoted  $\mathcal{SR}_{xy}$ , is inductively defined as follows: (i)  $xy \in \mathcal{SR}_{xy}$ ; (ii) If  $x'y' \in \mathcal{SR}_{xy}$ , then all its neighbor cells that are not limiting cells also belong to  $\mathcal{SR}_{xy}$ .

Table 2  
The limiting matrix  $M_{xy}^{\text{limit}}$  associated to a given region  $R$ .

	0	1	2	3	4	5	6	7	8	9	10	11	12	13	14	15
0	1	1	1	1	1	1	1	1	1	1	1	1	1	1	1	1
1	1	0	0	0	0	0	1	1	0	0	0	1	1	1	0	1
2	1	0	0	0	0	0	0	1	1	0	0	1	1	1	0	1
3	1	0	0	0	0	0	0	1	1	0	0	1	1	1	0	1
4	1	0	0	0	0	0	1	1	0	0	0	1	1	1	0	1
5	1	0	0	0	0	0	1	1	0	0	0	1	1	1	0	1
6	1	0	0	0	0	1	1	0	0	0	0	1	1	1	0	1
7	1	1	1	1	1	1	1	1	1	1	1	1	1	1	1	1

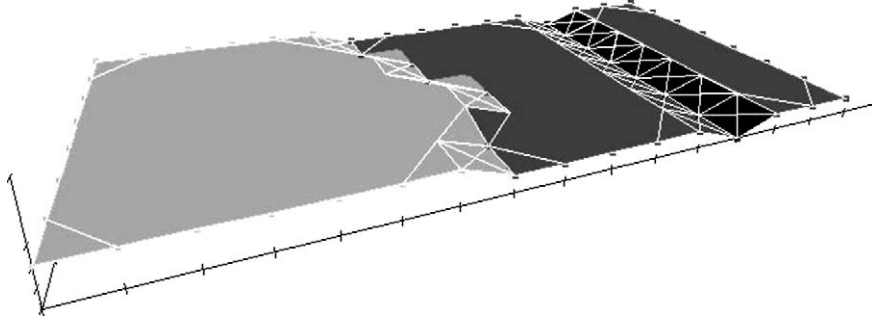


Figure 3. The declivity categorization of region  $R$ .

Observe that  $\mathcal{SR}_{xy} = \mathcal{SR}_{x'y'}$  if and only if  $x'y' \in \mathcal{SR}_{xy}$  (respectively,  $xy \in \mathcal{SR}_{x'y'}$ ). Definition 9 leads to a recursive algorithm similar to the ones commonly used to fulfill polygons. Table 2 shows the limiting matrix produced by the model in the categorization process<sup>5</sup> of a given region  $R$ . The related declivity categorization is shown in figure 3.

### 3. Conclusion

ICTM is a general tessellation-based model that is able to produce a reliable categorization of subregions of a given geographic region according to multiple characteristics known in sufficiently many points. The categorization determined by each characteristic is performed in one layer of the model, generating different subdivisions of the analyzed region. For instance, a region can be analyzed according to its topography, vegetation, demography, economic data, etc. The general tessellation-based model is not restricted to analyze bi-dimensional regions. The set of analyzed points may belong to a multi-dimensional space, determining the multi-dimensional character of each layer. A projection-like procedure of the categorization obtained in each layer into the base

<sup>5</sup> The numerical and graphical results were produced by the system Topo-ICTM.

layer will lead to a meaningful reliable categorization combining the analysis performed for each characteristic. This allows many interesting analysis on the mutual dependence of these characteristics.

In the case of Topo-ICTM, it considers just one characteristic, namely the declivity of the function that maps the relief of the considered region, performing a bi-dimensional analysis, which considers latitude and longitude. The dimension  $n_r \times n_c$  of the tessellation may be arbitrary or chosen according to specific criteria established by the application. In any case, the categorization obtained may be refined by either defining another tessellation dimension or taking each resulting subregion to be analyzed separately. The analysis may be performed until a convenient number of subregions is obtained, characterizing the dynamism of the model. The formalization using matrices of registers results that the information recorded in those registers is easily recovered by the indexing elements of the matrices, at any time. The implementation of the model is naturally parallel since the analysis is performed on the basis of local rules. As the input numeric data are usually susceptible to errors, interval arithmetic should be applied. Further work consists in the development of ICTM tools to support knowledge discovery based on categorization processes.

## Acknowledgements

The authors are very grateful to the Brazilian funding agencies CTPETRO/CNPq, CTINFO/CNPq and FAPERGS for their financial support and to the anonymous referees for their valuable suggestions.

## References

- [1] M.S. Aguiar, An interval  $n$ -dimensional  $m$ -layer categorizer tessellation model, Ph.D. thesis, PPGC/UFRGS, Brazil (2004) (in Portuguese).
- [2] D.D. Coblenz, V. Kreinovich, B.S. Penn and S.A. Tarks, Towards reliable subdivision of geological areas: Interval approach, in: *Soft Computing in Measurements and Information Acquisition*, eds. L. Reznik and V. Kreinovich (Springer, Berlin/Heidelberg, 2003) pp. 223–233.
- [3] M.C. Cooper, The tractability of segmentation and scene analysis, *Internat. J. Computer Vision* 30(1) (1998) 27–42.
- [4] K.S. Fu and J.K. Mui, A survey on image segmentation, *Pattern Recognition* 13(1) (1981) 3–16.
- [5] R.B. Kearfort and V. Kreinovich, eds., *Applications of Interval Computations* (Kluwer, Dordrecht, 1996).
- [6] J.L. Lisani, L. Moisan, P. Monasse and J.M. Morel, On the theory of planar shape, *Multiscale Modeling Simulation* 1(1) (2003) 1–24.
- [7] R.E. Moore, *Methods and Applications of Interval Analysis* (SIAM, Philadelphia, PA, 1979).
- [8] S.E. Umbaugh, *Computer Vision and Image Processing* (Prentice-Hall, Upper Saddle River, NJ, 1998).
- [9] K. Villaverde and V. Kreinovich, A linear-time algorithm that locates local extrema of a function of one variable from interval measurements results, *Interval Computations* 4 (1993) 176–194.